Soft Chemical Dehydration Route to Carbon Coating of Metal Oxides: Its Application for Spinel Lithium Manganate

Ah Reum Han, Tae Woo Kim, Dae Hoon Park, Seong-Ju Hwang,* and Jin-Ho Choy*

Center for Intelligent Nano-Bio Materials, Division of Nano Sciences and Department of Chemistry, Ewha Womans University, Seoul 120-750, Korea

Received: March 30, 2007; In Final Form: May 28, 2007

On the basis of the dehydration reaction of carbohydrate molecules assisted by sulfuric acid, we have invented a novel soft chemical route to the carbon coating of metal oxides. As a representative, this technique has been applied to the carbon coating of spinel $LiMn_2O_4$ electrode material for lithium secondary batteries. Electron microscopy, elemental analysis, and N_2 adsorption−desorption isotherm measurements clearly demonstrate that porous carbon nanolayer with the thickness of ∼10−25 nm is successfully coated by the dehydration reaction of sucrose-adsorbed lithium manganese oxide at 90 °C. According to power X-ray diffraction, Mn K-edge X-ray absorption, and micro-Raman spectroscopic analyses, the carbon coating does not modify the cubic spinel-type atomic arrangement of lithium manganate, while the coated carbon layer is composed of disordered amorphous carbon and polycyclic aromatic hydrocarbons. Of special importance is that the carbon coating can improve the electrode performance of spinel lithium manganate, which would be attributed to the increase of grain connectivity and/or to the protection of manganese oxide from chemical corrosion. This interpretation is further supported by the acid corrosion test showing that the dissolution of Mn ions in an acidic medium is remarkably depressed by the carbon coating. On the basis of the present experimental findings, we are able to conclude that the low-temperature dehydration method provides a novel, less energy-consuming route to the carbon coating of diverse metal oxides.

Introduction

Over the last decades, intense research activities have been concentrated on transition metal oxides because of their wide applications as electrodes, catalysts, ionic conductors, magnetic materials, and so on.[1−3] The physicochemical properties of the transition metal oxides can be controlled through diverse manipulations such as chemical substitution, surface coating, and the hybridization between different metal oxides.[4−8] In particular, a carbon coating has been known to be effective not only in enhancing the electrical conductivity of metal oxides but also in increasing their absorbing ability against organic molecules. In addition, a coated carbon layer would protect the metal oxides from chemical corrosion. For this reason, there have been many studies about the carbon coating for various transition metal oxides including electrode materials for lithium secondary batteries and photocatalysts.[5,6,8,9] As a consequence, diverse methods of carbon coating such as chemical vapor deposition, pyrolysis of polymeric carbon precursors, sol−gel synthesis, and hydrothermal decomposition of adsorbed organic precursors have been developed.[5,6,8−11] To date, however, most of the methods reported contain a heat-treatment step at elevated temperature and/or require special apparatus like a deposition machine, which would increase the energy consumption and the production cost of carbon-coated metal oxides. In this regard, the exploration of a less energy-consuming route of carbon coating has remained as a challenging issue for chemists and material scientists.

In the present work, we have developed a novel soft chemical carbon-coating method and demonstrated its usefulness through the carbon-coating of spinel lithium manganate. This method is based on the low-temperature dehydration of sucrose molecules assisted by sulfuric acid.[12] The crystal structure, carbon content, and surface area of carbon-coated lithium manganates were examined with powder X-ray diffraction (XRD), elemental CHNS analysis, and N_2 adsorption−desorption isotherm measurements. We have investigated their crystallite morphology and chemical bonding nature using transmission electron microscopy (TEM), field emission-scanning electron microscopy (FE-SEM), micro-Raman spectroscopy, and Mn K-edge X-ray absorption spectroscopy (XAS). In addition, the influences of the carbon coating on the electrode performance and Mn leaching behavior of the spinel $LiMn_2O_4$ compound have been investigated.

Experimental Section

Sample Preparation. The spinel $LiMn_2O_4$ sample was prepared by heating the stoichiometric mixture of Li_2CO_3 and Mn_2O_3 at 750 °C for 24 h with intermittent grindings.[13] Carbon coating for $LiMn_2O_4$ was carried out by the sulfuric acid-assisted dehydration reaction of adsorbed sucrose molecules, as illustrated in Figure 1. First, the pristine $LiMn_2O_4$ was soaked in the aqueous solution of sucrose and sulfuric acid and then heated at 90 °C for 12 h in air for the dehydration of surface-adsorbed sucrose molecules. The weight fraction of sucrose with respect to $LiMn_2O_4$ was controlled to be 1/20 (in which case the obtained sample is denoted as **C1**), 1/10 (here the obtained sample is denoted as **C2**), or 1/5 (here the obtained sample is denoted as **C3**), whereas the mole ratio of sulfuric acid to $LiMn_2O_4$ was fixed at 1/330 for all the present samples. The adsorbed solvent was removed by heat treatment at 90 °C for 4 h under vacuum, and the resulting samples were further

* To whom correspondence should be addressed: tel +82-2-3277-4370; fax +82-2-3277-3419; e-mail hwangsju@ewha.ac.kr.

10.1021/jp0725230 CCC: $37.00
Published on Web 07/11/2007

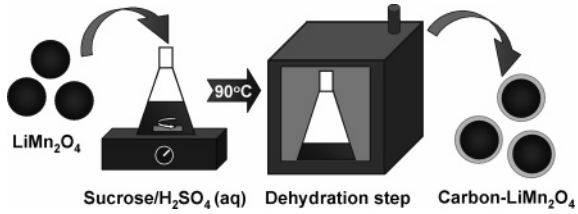

Figure 1. Schematic diagram for the low-temperature dehydration route to carbon coating of lithium manganese oxide.

dried for several weeks in a closed container with desiccants. In addition, free carbon was prepared as a reference through the dehydration of aqueous sucrose−sulfuric acid solution under the same condition applied for the coating of the spinel electrode materials.

Sample Characterization. The variation of the crystal structure of $LiMn_2O_4$ upon the carbon coating was studied by powder XRD with Ni-filtered Cu Kα radiation and a graphite diffracted beam monochromator. The content of coated carbon was determined by elemental CHNS analysis as 3.3%, 6.8%, and 8.0% for **C1**, **C2**, and **C3**, respectively. The morphology and thickness of the coated carbon layer were examined with FE-SEM and TEM measurements. The effect of carbon coating on the surface area of lithium manganate was examined by measuring volumetrically nitrogen adsorption−desorption isotherms at liquid nitrogen temperature. The samples were degassed at 100 °C for 2 h under vacuum before the adsorption measurement. Micro-Raman spectra presented here were recorded on a Renishaw instrument coupled with an optical microscope (spatial resolution of 1 μm^2). The samples were excited with the 514.5 nm line of an Ar^+ laser. All the present spectra were obtained by backscattering from the powdered sample. XAS experiments were carried out at Mn K-edge by using the extended X-ray absorption fine structure (EXAFS) facility installed at beam line 7C of the Pohang Accelerator Laboratory (PAL) in Korea, operated at 2.5 GeV and 180 mA. XAS data were collected at room temperature in transmission mode by use of a Si(111) single-crystal monochromator and gas-ionization detectors. All the present spectra were calibrated carefully by measuring the reference spectrum of Mn metal simultaneously. Data analysis for the experimental spectra was carried out by the standard procedure.[14] In the course of EXAFS fitting analysis, the coordination number (*CN*) was fixed to the crystallographic values while the amplitude reduction factor (S_0^2) was allowed to vary. The best-fit S_0^2 values of both the lithium manganates are consistent with each other within 10% deviation. All the bond distances (*R*), Debye−Waller factors (σ^2), and energy shifts (ΔE) were set as variables. The electrochemical measurements were performed with the cell of Li/1 M $LiPF_6$ in EC/DEC (50:50 v/v) composite cathode, which was assembled in a drybox. The composite cathode was prepared by mixing thoroughly the active $LiMn_2O_4$ cathode material (85%) with 10% acetylene black and 5% PTFE [poly(tetrafluoroethylene)]. All the experiments were carried out in a galvanostatic mode with constant current density of 0.5 mA/cm^2 in the voltage range of 3.5−4.3 V. In addition, the leaching of manganese ions from the pristine spinel lithium manganate and its carbon-coated derivatives was monitored in an acidic medium. The acid corrosion test was carried out by reacting 2.00−2.17 g of the electrode materials with 100 mL of 0.2 M HCl aqueous solution at room temperature for 6 h. Due to the presence of coated carbon species, a larger amount of the samples was used for the carbon-coated derivatives compared to the uncoated lithium manganate. This makes the same amount of manganese ions subjected to acid leaching for all cases. After the acid treatments, the concentration of manganese ions in the supernatant solution was analyzed with inductively coupled plasma (ICP) spectrometry.

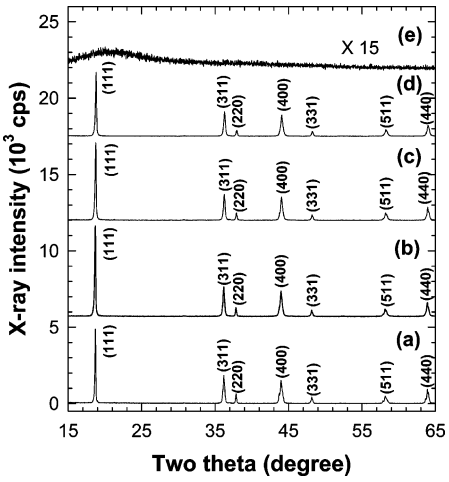

Figure 2. Powder XRD patterns of (a) the pristine $LiMn_2O_4$, its carbon-coated derivatives (b) **C1**, (c) **C2**, and (d) **C3**, and (e) free carbon synthesized from the dehydration of sucrose.

TABLE 1: Lattice Parameter, Unit Cell Volume, and Crystal Symmetry of Spinel Lithium Manganate and Its Carbon-Coated Derivatives

compd	*a* (Å)	V_c	crystal symmetry
$LiMn_2O_4$	8.2458	560.658	cubic
C1	8.2445	560.393	cubic
C2	8.2421	559.904	cubic
C3	8.2328	558.011	cubic

Results and Discussion

Powder XRD Analysis. The powder XRD patterns of the pristine $LiMn_2O_4$ and its carbon-coated derivatives are plotted in Figure 2, in comparison with that of free carbon prepared from the dehydration of sucrose. Regardless of the carbon coating, all the present lithium manganates show nearly identical diffraction patterns with sharp Bragg reflections. There is only a negligible dependence of peak intensity and position on the carbon content. The present XRD patterns can be well indexed on the basis of cubic spinel structure with the space group of *Fd*-3*m*,[13] indicating that the carbon coating has little influence on the cubic spinel-type atomic arrangement of the lithium manganate. The lattice parameters and unit cell volumes of all the spinel oxides were calculated from the least-squares fitting analysis. As listed in Table 1, the carbon coating causes a slight contraction of unit cell volume, reflecting the partial oxidation of manganese ions by incorporated sulfuric acid. On the other hand, the free carbon obtained from the dehydration of the sucrose does not display any distinct diffraction peaks, indicative of its X-ray amorphous nature.

Electron Microscopy and N_2 Adsorption−Desorption Isotherm Analyses. The effect of carbon coating on the crystallite morphology of the spinel $LiMn_2O_4$ was examined by FE-SEM. As illustrated in Figure 3, the pristine lithium manganate and its carbon-coated derivative commonly exhibit irregular polyhedral morphology with particle sizes of ~0.5−3 μm. Although the carbon coating does not induce any marked change in the shape and size of the $LiMn_2O_4$ crystallites, the carbon-coated material displays smoother surface than the pristine compound, suggestive of the deposition of uniform carbon layer. The coating of carbon nanolayers on the surface of the spinel crystallites was further confirmed by TEM analysis,

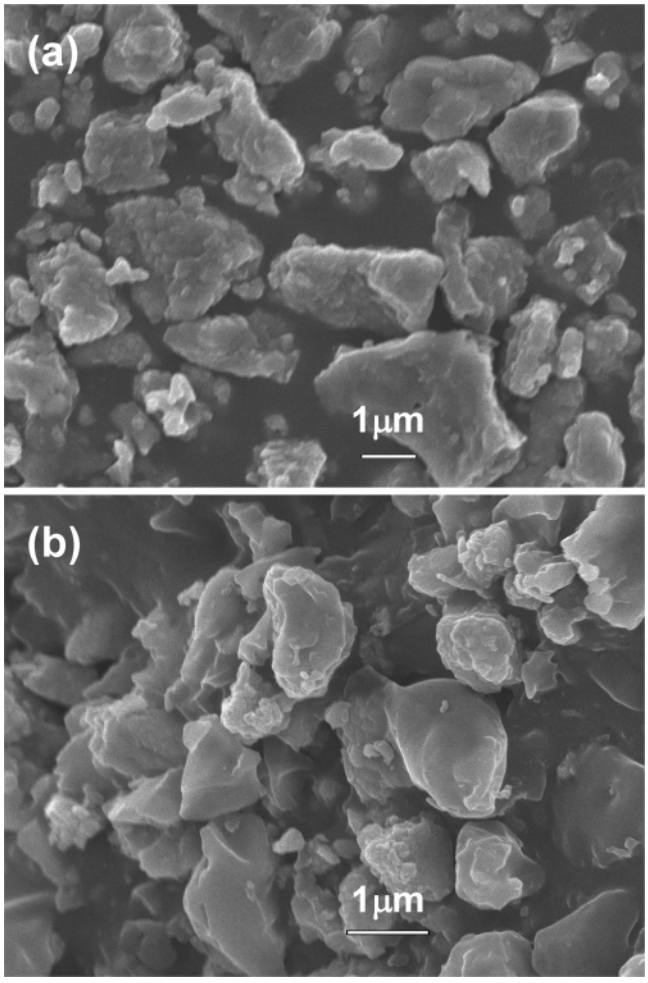

Figure 3. FE-SEM images of (a) pristine $LiMn_2O_4$ and (b) its carbon coated derivative, **C3**.

as presented in Figure 4. The dark part in the present images represents the microcrystals of spinel lithium manganate while the bright part on the edge of spinel crystallites corresponds to the coated carbon layer. The contrast of each part originates from their relative density. As illustrated in Figure 4, carbon layer with an average thickness of ~10−25 nm is coated on the surface of lithium manganese oxide. Due to their high carbon contents, heavily carbon coated derivatives show the partial formation of isolated carbon grains. As the amount of coated carbon increases, the coated layer becomes thicker. The average thickness of coated carbon layers was estimated to be ~10 nm for **C1**, ~20 nm for **C2**, and ~25 nm for **C3**, which indicates that the thickness of the coated carbon layer can be controlled by changing the ratio between sucrose and $LiMn_2O_4$. The electron microscopic results presented here clearly demonstrate that the low-temperature dehydration method is effective in forming a carbon nanolayer on the surface of metal oxide. Also, we have examined the variation of surface area upon carbon coating by performing N_2 adsorption−desorption isotherm measurements. The carbon coating increases the small surface area of the pristine $LiMn_2O_4$ (1.4 m^2/g) to 6.5 m^2/g for **C3**, indicative of the porous nature of coated carbon layers.

Mn K-Edge XANES Analysis. The evolution of the chemical bonding nature of manganese ions upon the carbon coating has been studied by Mn K-edge X-ray absorption near-edge structure (XANES) analysis. Figure 5 represents the Mn K-edge XANES spectra for pristine $LiMn_2O_4$ and its carbon-coated derivatives, in comparison with the reference spectra of layered $LiMn^{III}_{0.9}Cr_{0.1}O_2$, $Mn^{III}_2O_3$, and $Mn^{IV}O_2$. The edge jump of $LiMn_2O_4$ is observed midway between those of the references Mn_2O_3 and MnO_2, which is in good agreement with the mixed oxidation state of manganese ions in this compound.[13] All the present samples show weak pre-edge peaks P and P′ corresponding to dipole-forbidden 1s → 3d transitions.[15] Despite the violation of the electronic selection rule ($\Delta l = \pm 1$), these features can be observed due to the mixing of 4p and 3d states. If it is taken into account that such mixing is hard to achieve in the centrosymmetric octahedral geometry, the weak intensity of the pre-edge peaks strongly suggests that all the manganese ions in $LiMn_2O_4$ and its carbon-coated derivatives exist in the octahedral site of spinel lattice. A close inspection of the pre-edge spectra reveals that the reference MnO_2 with tetravalent manganese ions displays a stronger intensity of P′ than P, whereas only one feature P at lower energy appears for trivalent manganese oxides; see the inset of Figure 5. Two peaks, P and P′, are discernible commonly for the spectra of the spinel lithium manganate and its carbon-coated derivatives. But the intensity of the peak P′ is weaker for these compounds than for the reference MnO_2. Since the intensity of the peak P′ is proportional to the Mn oxidation state,[15] this observation confirms the mixed oxidation state of Mn^{III}/Mn^{IV} in these compounds. In the main-edge region, there are several features corresponding to the dipole-allowed transitions from core 1s to the unoccupied 4p levels. Among them, the peak A has been assigned as 1s → $4p_\pi$ transition with a shakedown process.[4] Due to the sensitivity of the shakedown process to the electrostatic repulsion between $4p_\pi$ orbital and axial ligands, the intensity of peak A can provide a sensitive indicator for probing a local structural distortion around the manganese ion.[4] As shown in Figure 5, the layered $LiMn_{0.9}Cr_{0.1}O_2$ phase exhibits a very strong peak A, since the Jahn−Teller- (JT-) active trivalent manganese ion in this compound is stabilized in the tetragonally distorted octahedra. Regardless of the carbon coating, all the spinel compounds show only a weak peak A, clearly demonstrating the absence of local structural deformation caused by the carbon coating. On the other hand, the carbon coating enhances notably the spectral weight of peak C. Judging from the fact that the intensity of this feature is proportional to the Mn oxidation state

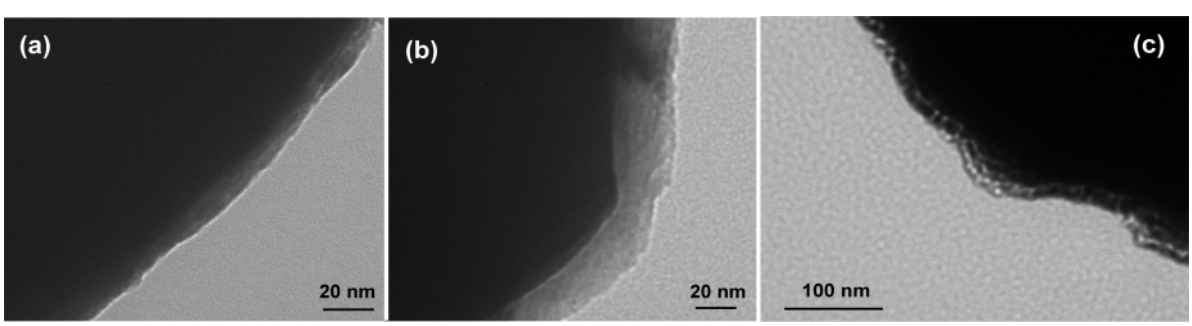

Figure 4. TEM images of the carbon-coated $LiMn_2O_4$: (a) **C1**, (b) **C2**, and (c) **C3**.

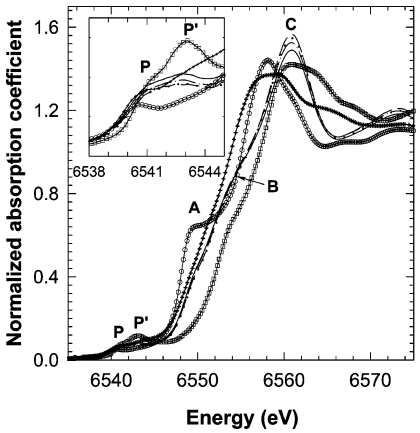

Figure 5. Mn K-edge XANES spectra for the pristine $LiMn_2O_4$ (—), its carbon-coated derivatives **C1** (···), **C2** (— — —), and **C3** (— · —), in comparison with those for Mn_2O_3 (+), $LiMn_{0.9}Cr_{0.1}O_2$ (○), and MnO_2 (□). (Inset) Enlarged views of all the present spectra with an energy range of 6538−6545 eV.

in the spinel lattice,[16] the observed enhancement of peak C upon carbon coating can be regarded as a proof of the oxidation of manganese ions.[16]

Mn K-Edge EXAFS Analysis. We have tried to quantitatively determine the variation of Mn local structure upon carbon coating by use of Mn K-edge EXAFS analysis. The Fourier transforms (FTs) of k^3-weighted Mn K-edge EXAFS spectra for $LiMn_2O_4$ and its carbon-coated derivative (**C3**) are plotted in Figure 6a and the corresponding Fourier-filtered oscillations in Figure 6b, respectively. Both the compounds commonly display two FT peaks corresponding to the Mn−O and Mn−Mn shells at ∼1.6 and ∼2.6 Å. Before and after the carbon coating, the EXAFS data of $LiMn_2O_4$ remain basically the same in the *R*- and *k*-spaces. As presented in Figure 6b, all of the present EXAFS data could be well reproduced on the basis of the cubic spinel structure with a regular MnO_6 octahedron with six neighboring manganese ions at the same distance.[17] As listed in Table 2, the manganese ions in the as-prepared $LiMn_2O_4$ compound are coordinated by six oxygen ligands at 1.90 Å and six manganese ions at 2.84 Å. Upon the carbon-coating process, the bond distances of Mn−O and Mn−Mn become shorter by 0.01−0.02 Å. Although the decrease of bond lengths is within or close to the error limit of EXAFS analysis ($\Delta R = \pm 0.01$ Å), the present EXAFS results seem to reflect the partial oxidation of manganese ion. This is in good agreement with the XRD and XANES results revealing the contraction of unit cell volume and the increase of Mn oxidation state upon carbon coating. As listed in Table 2, the coordination numbers and Debye−Waller factors are very similar for both spinel compounds, strongly suggesting the absence of structural disorder caused by carbon coating. To summarize the present EXAFS fitting results, the cubic spinel structure of $LiMn_2O_4$ is well maintained during the carbon coating process but the bond distances of Mn−O and Mn−Mn are slightly shortened.

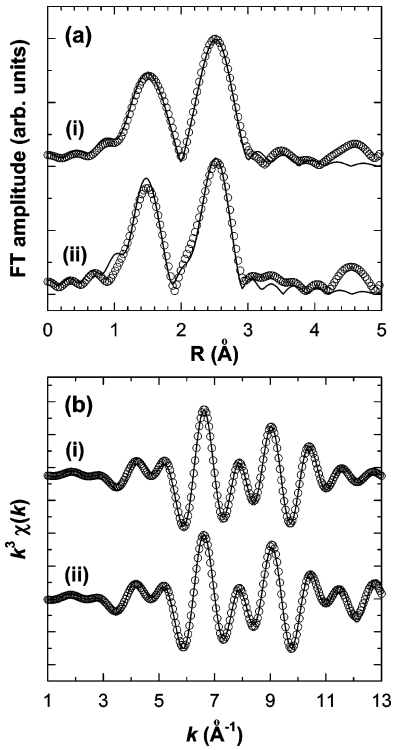

Figure 6. (a) Fourier-transformed and (b) Fourier-filtered Mn K-edge EXAFS spectra for (i) pristine $LiMn_2O_4$ and (ii) its carbon-coated derivative, **C3**.

Micro-Raman Analysis. The chemical bonding character of carbon species coated on lithium manganate has been investigated with micro-Raman spectroscopy. Figure 7 represents micro-Raman spectra of the pristine $LiMn_2O_4$ and its carbon-coated derivative in the frequency region of 1100−1800 cm^{-1}. Since the low content and high conductivity of carbon species coated on $LiMn_2O_4$ cause weak Raman signals with poor signal-to-noise (S/N) ratio, we have also measured micro-Raman spectrum of the free carbon obtained from the dehydration of sucrose. Due to the same synthetic conditions, the free carbon is believed to have basically the same bonding nature as the coated carbon layer. As shown in Figure 7, the free carbon shows two distinct peaks in the present wavenumber region, which are typical of disordered amorphous carbon.[9,18,19] In fact, similar features were observed in the Raman spectra of the carbon-coated alumina prepared by pyrolysis of sucrose-coated alumina at 600 °C.[9] This confirms that the present low-temperature method produces amorphous carbon layers similar to the carbon species synthesized by the high-temperature pyrolysis route. The observed peaks at 1365 and 1585 cm^{-1} can be assigned as the D and G phonon lines, corresponding to the bond stretching mode of all pairs of sp^2 atoms in rings and chains and the breathing mode of bonded carbon in rings, respectively.[18] It was reported that the full width at half maximum (fwhm) of peak G is proportional to the degree of disorder in carbon species.[18] The higher energy peak G exhibits

TABLE 2: Results of Nonlinear Least-Squares Curve Fittings for the Mn K-Edge EXAFS Spectra of Cubic Spinel $LiMn_2O_4$ and Its Carbon-Coated Derivative, C3

compd	bond	CN	ΔE (eV)	R (Å)	σ^2 (10^{-3} Å)
$LiMn_2O_4$[a]	Mn−O	6	−2.28	1.90	4.50
$LiMn_2O_4$[a]	Mn−Mn	6	−2.68	2.90	4.53
carbon−$LiMn_2O_4$[b]	Mn−O	6	−7.51	1.88	3.92
carbon−$LiMn_2O_4$[b]	Mn−Mn	6	−5.25	2.89	5.06

[a] The curve-fit was performed for $R = 0.982-2.884$ Å and $k = 3.80-11.70$ $Å^{-1}$. [b] The curve-fit was performed for $R = 1.043-2.853$ Å and $k = 3.75-13.00$ $Å^{-1}$.

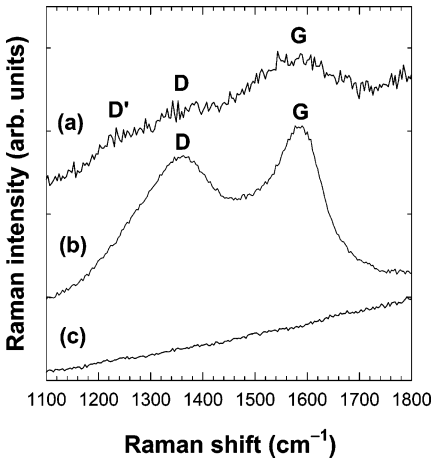

Figure 7. Micro-Raman spectra of (a) carbon-coated $LiMn_2O_4$ (**C3**), (b) free carbon synthesized from the dehydration of sucrose, and (c) pristine $LiMn_2O_4$.

a wider fwhm of ~150 cm^{-1} for the free carbon than for graphitic carbon,[18] implying the presence of significant disorder in the coated carbon species. In addition, an appearance of the broad peak D at lower energy can be regarded as evidence of the presence of several types of polycyclic aromatic hydrocarbons with different vibration frequencies.[19] Even with poor S/N ratio, the carbon-coated $LiMn_2O_4$ material shows Raman spectral features similar to those of the free carbon (Figure 7). Besides, an additional broad peak denoted as D′ is detected at lower energy for the carbon-coated $LiMn_2O_4$, indicating that polycyclic aromatic hydrocarbons in the coated carbon layer of this metal oxide possess more versatile chemical bonding character than those in the free carbon. This spectral feature would be a result of the significant interaction of hydrocarbons with the surface of metal oxide. In fact, a similar peak was discernible at around 1200 cm^{-1} in the Raman spectra of the carbon-coated alumina synthesized by the pyrolysis of adsorbed sucrose.[9] On the other hand, in the low wavenumber region of 200−700 cm^{-1}, the pristine material and its carbon-coated derivative display commonly characteristic phonon lines of cubic spinel $LiMn_2O_4$ lattice, which confirms negligible variation of crystal structure upon carbon coating. In this regard, the present Raman results can provide strong evidence for the formation of coated carbon layers without significant modification of the spinel lattice.[9]

Electrochemical Measurements. We have studied the influence of carbon coating on the cathode performance of spinel lithium manganates for lithium secondary batteries. The discharge capacities of pristine $LiMn_2O_4$ and its carbon-coated derivatives are plotted in Figure 8 as a function of cycle number. In comparison with pristine $LiMn_2O_4$, the carbon-coated materials show larger discharge capacity in the entire cycle range, underscoring the effectiveness of the present coating method in improving the electrochemical performance of electrode materials. In particular, the lightly carbon-coated material **C1** exhibits the most promising electrode performance. With reference to TEM results, this finding indicates that the coating of carbon layers with a thickness of ~10 nm is effective in improving the electrochemical performance of spinel electrode materials. Such a positive effect of carbon coating is in good agreement with the previous report on carbon-coated compound prepared by high-temperature carbonization process.[5,6] Judging from the conductive nature of coated carbon layers, the superior performance of the carbon-coated material is attributable to enhancement of electronic connection between lithium manganate grains, preventing the formation of electrically short-circuited domains. On the other hand, it has been well-known

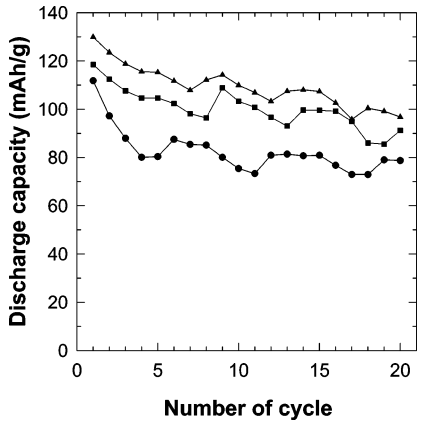

Figure 8. Discharge capacities of pristine $LiMn_2O_4$ (●) and its carbon coated derivatives **C1** (▲) and **C2** (■) as a function of cycle number.

that surface Mn^{III} ions of manganese oxides are easily disproportionated into Mn^{IV} and Mn^{II} ions through the contact with electrolyte.[16,20,21] The leaching of soluble Mn^{II} ions from the electrode into the solution also makes a significant contribution to the capacity fading of spinel oxides. Considering the fact that the carbon coating can protect the spinel electrode from direct contact with electrolytes, the prevention of Mn dissolution during electrochemical cycling would be partially responsible for better electrode performance of the carbon-coated compound.

Acid Corrosion Tests. To confirm this speculation, we have examined the leaching of manganese ions from pristine $LiMn_2O_4$ and its carbon-coated derivatives in an acidic medium by monitoring the manganese concentration in supernant solution. According to the ICP analysis, the molar concentration of manganese ions leached from the pristine compound was estimated to be 0.067 M. Of special interest is that the carbon coating depresses remarkably the dissolution of Mn ions to 0.008−0.011 M. Although the increase of coated carbon content decreases the concentration of manganese ions dissolved, the difference of Mn concentration in the supernant solution is not large from **C1** to **C3**. This implies that the coating with the lowest carbon content (i.e., **C1**) is sufficient for protection of the spinel lattice from acidic corrosion. Furthermore, the negligible dissolution of Mn ions from all the carbon-coated compounds can be regarded as another evidence of the formation of uniformly coated carbon layers via the present dehydration route. To summarize the experimental findings, the dehydration route of carbon coating is very effective in preventing the dissolution of manganese ions from the spinel lattice as well as in enhancing the electrode performance of the spinel $LiMn_2O_4$.

Conclusions

In this study, we have successfully developed a novel soft chemical carbon-coating method based on the dehydration reaction of sucrose molecules assisted by sulfuric acid. With this method, a porous carbon nanolayer with thickness ~10−25 nm can be coated uniformly on spinel-structured lithium manganate. According to power XRD and Mn K-edge XANES/EXAFS analyses, the carbon coating does not frustrate the spinel-type structure of pristine $LiMn_2O_4$ but slightly enhances the average oxidation state of manganese ions. Micro-Raman spectroscopic results clearly demonstrate that the coated carbon species are in the form of disordered amorphous carbons and/or polycyclic aromatic hydrocarbons. Of special importance is that the carbon-coated lithium manganates show better electrode performance compared to the uncoated pristine material, which would stem from enhancement of the chemical stability of spinel

lithium manganate and/or from increased grain connectivity. In this regard, one can conclude that the present method provides a novel, less energy-consuming route not only to carbon coating of metal oxides but also to improvement of electrode performance. When the porous nature of formed carbon layers is taken into account, the low-temperature dehydration route is supposed to be more suitable for the carbon coating of anode or catalyst materials.[7,10] In light of this, our current project is application of the present method to other metal oxides used as anodes for Li^+ ion batteries or as heterogeneous photocatalysts.

Acknowledgment. This work was supported by a grant (20070401034003) from the BioGreen 21 Program and partly by the SRC/ERC program of MOST/KOSEF (Grant R11-2005-008-03002-0). The experiments at Pohang Accelerator Laboratory (PAL) were supported in part by MOST and POSTECH.

References and Notes

(1) Thackeray, M. M. *Prog. Solid State Chem.* **1997**, *25*, 1.

(2) Hoffmann, M. R.; Martin, S. T.; Choi, W.; Bahnemann, D. W. *Chem. Rev.* **1995**, *95*, 69.

(3) Hur, S. G.; Park, D. H.; Kim, T. W.; Hwang, S.-J. *Appl. Phys. Lett.* **2004**, *85*, 4130.

(4) (a) Hwang, S.-J.; Park, H. S.; Choy, J. H.; Campet, G. *J. Phys. Chem. B* **2000**, *104*, 7612. (b) Hur, S. G.; Kim, T. W.; Hwang, S.-J.; Park, H.; Choi, W.; Kim, S. J.; Choy, J.-H. *J. Phys. Chem. B* **2005**, *109*, 15001. (c) Lim, S. T.; Park, D. H.; Lee, S. H.; Hwang, S.-J.; Yoon, Y. S.; Kang, S. G. *Bull. Kor. Chem. Soc.* **2006**, *27*, 1310.

(5) (a) Cho, J.; Kim, C.; Park, B. *J. Electrochem. Soc.* **2001**, *148*, A1110. (b) Cushing, B. L.; Goodenough, J. B. *Solid State Sci.* **2002**, *4*, 1487.

(6) (a) Cao, Q.; Zhang, H. P.; Wang, G. J.; Xia, Q.; Wu, Y. P.; Wu, H. Q. *Electrochem. Commun.* **2007**, *9*, 1228. (b) Chin, H. C.; Cho, W. I.; Jang, H. *Electrochim. Acta* **2006**, *52*, 1472.

(7) (a) Inagaki, M.; Kojin, F.; Tryba, B.; Toyoda, M. *Carbon* **2005**, *43*, 1652. (b) Zheong, T.; Dong, Y.-R.; Nishiyama, N.; Egashira, Y.; Ueyama, K. *Appl. Catal., A* **2006**, *308*, 210.

(8) (a) Kim, T. W.; Hur, S. G.; Hwang, S.-J.; Choy, J. H. *Chem. Commun.* **2006**, *220*. (b) Park, H. M.; Kim, T. W.; Hwang, S.-J.; Choy, J. H. *Bull. Kor. Chem. Soc.* **2006**, *27*, 1323.

(9) Lin, L.; Lin, W.; Zhu, Y. X.; Zhao, B. Y.; Xie, Y. C.; Jia, G. Q.; Li, C. *Langmuir* **2005**, *21*, 5040.

(10) Noh, M.; Kwon, Y.; Lee, H.; Cho, J.; Kim, Y.; Kim, M. G. *Chem. Mater.* **2005**, *17*, 1926.

(11) (a) Dominko, R.; Gaberscek, M.; Drofenik, J.; Bele, M.; Pejovnik, S. A. *Electrochem. Solid State Lett.* **2001**, *4*, A187. (b) Sharma, N.; Shaju, K. M.; Subba Rao, G. V.; Chowdari, B. V. R.; Dong, Z. L.; White, T. J. *Chem. Mater.* **2004**, *16*, 504.

(12) Ryoo, R.; Joo, S. H.; Ju, S. *J. Phys. Chem. B* **1999**, *103*, 7743.

(13) Hwang, S.-J.; Park, H. S.; Choy, J.-H.; Campet, G. *J. Phys. Chem. B* **2001**, *105*, 335.

(14) Choy, J.-H.; Hwang, S.-J.; Park, N. G. *J. Am. Chem. Soc.* **1997**, *119*, 1624.

(15) Treuil, N.; Labrugère, C.; Menetrier, M.; Portier, J.; Campet, G.; Deshayes, A.; Frison, J. C.; Hwang, S.-J.; Song, S.-W.; Choy, J.-H. *J. Phys. Chem. B* **1999**, *103*, 2100.

(16) Ammundsen, B.; Jones, D. J.; Rozière, J.; Burns, G. R. *Chem. Mater.* **1996**, *8*, 2799.

(17) The best-fitted residual F^2 factor ($= \Sigma\{k^3(\chi(k)_{cal} - \chi(k)_{exp})\}^2/(n - 1)$, n is the number of data) was determined to be 0.041 for $LiMn_2O_4$ and 0.057 for the carbon-coated derivative.

(18) Ferrari, A. C.; Robertson, J. *Phys. Rev. B* **2001**, *64*, 075414.

(19) Negri, F.; Castiglioni, C.; Tommasini, M.; Zerbi, G. *J. Phys. Chem. A* **2002**, *106*, 3306.

(20) Gummow, R. J.; de Kock, A.; Thackeray, M. M. *Solid State Ionics* **1994**, *69*, 59.

(21) Thackeray, M. M.; Mansuetto, M. F.; Bates, J. B. *J. Power Sources* **1997**, *68*, 153.